

DESIGN AND HARDWARE IMPLEMENTATION OF MODIFIED INCREMENTAL CONDUCTANCE ALGORITHM FOR PHOTOVOLTAIC SYSTEM

Djamel OUNNAS , Dhaouadi GUIZA , Youcef SOUFI , Mahmoud MAAMRI 

LABGET Laboratory, Department of Electrical Engineering, Faculty of Science and Technology,
University of Tebessa, Route de Constantine, 12002 Tebessa, Algeria

djamel.ounnas@univ-tebessa.dz, dhaouadi.guiza@univ-tebessa.dz, soufi.youcef@univ-tebessa.dz,
mahmoud.maamri@univ-tebessa.dz

DOI: 10.15598/aeee.v19i2.3881

Article history: Received Jul 18, 2020; Revised Jan 25, 2021; Accepted Mar 19, 2021; Published Jun 30, 2021.
This is an open access article under the BY-CC license.

Abstract. *This paper deals with the design, simulation and real-time implementation of Maximum Power Point Tracking (MPPT) technique for a Photovoltaic (PV) system. A new modified Incremental Conductance (INC) algorithm is proposed to extract maximum power from PV panels at different levels of temperature and solar irradiation. The considered PV system consists of a PV panel, a DC-DC boost converter controlled by MPPT algorithm and a resistive load. First, the simulation tests of the proposed algorithm using Matlab/Simulink environment are presented, and then, followed by a real-time implementation using Arduino Mega board and a specific package known as “Simulink support package for arduino hardware” to validate experimentally the simulation tests. Simulation and experimental results show that the proposed modified INC algorithm offers much less oscillation around the Maximum Power Point (MPP), fast dynamic response and better performances compared to the conventional INC algorithm.*

Keywords

Arduino board, MPPT, PV system, Simulink support package for Arduino hardware.

1. Introduction

Recently, the demand for electrical energy has increased, and so the effects of its production, such as the global warming and pollution. Therefore,

the search for alternative energy sources has become a worldwide effort. Many scientists are working on different ways to find a substitute for the traditional fossil fuel of gas, oil and coal sources by renewable energies [1], [2], and [3]. In this context, PV panels offer a very competitive solution since they directly convert sunlight into electrical energy without any noise pollution and do not involve any moving part [4]. However, their main drawbacks are the low efficiency and their nonlinear power-voltage characteristic which depends on atmospheric conditions, particularly solar irradiation and temperature [5] and [6].

To extract maximum power from PV panels at different levels of temperature and solar irradiation, it is necessary to add, between the PV panel and the load, a DC-DC converter controlled by an MPPT algorithm. This leads to force the PV panel to operate at its maximum power point, irrespective of changing atmospheric conditions [7] and [8]. Many MPPT control algorithms have been developed since the 1970s, among which we can cite the conventional controllers such as Hill Climbing (HC) [9] and [10], Perturb and Observe (P&O) [11] and [12] and Incremental Conductance (INC) [13] and [14]. However, these algorithms suffer from some drawbacks.

To address and overcome the shortcomings of conventional methods, many MPPT techniques have been proposed based on artificial intelligence approaches, such as Fuzzy Logic Control (FLC) [15] and [16], Adaptive Neuro-Fuzzy Inference System (ANFIS) [17] and [18], optimized adaptive control [19], Genetic Algorithm Optimization (GAO) [20], Teaching-Learning-Based Optimization (TLBO) [21], backstepping con-

trol [22] and Particle Swarm Optimization (PSO) [23] and [24], silver mean method [25]. For example, in [15], an FLC has been combined with the conventional P&O algorithm to design a new MPPT-based controller that has fast time response, less overshoot and more stable operation. On the other hand, in [16], the voltage and power outputs have been used as inputs for an FLC-based MPPT controller to produce the appropriate Pulse Width Modulation (PWM) signal to the DC-DC converter. It can also be shown that the results in [17], [18], [19], and [20] show good performance in terms of efficiency and rapidity.

The simulation results of the MPPT-based advanced control techniques have been proved to be effective and successful in the extraction of maximum power from PV panels. Nevertheless, the main challenge facing these techniques is usually the practical implementation stage. Furthermore, they may often require several sensors thereby increasing the cost of control systems. For instance in [5], the real-time implementation of the proposed Takagi-Sugeno-based MPPT method needs temperature sensor, solar irradiation sensor, two voltage sensors and two current sensors. However, by using conventional methods such as P&O and INC, only two sensors (voltage and current sensors) are required to implement practically each of these algorithms.

In recent years, many researchers have proposed new MPPT algorithms based on conventional INC to benefit from its simplicity, to overcome its drawbacks, and to improve its performance [26], [27], [28], [29], and [30]. The first drawback of conventional INC algorithm resides in the choice of the step size. If it is large, the algorithm will find the MPP rapidly, but in this case, considerable fluctuations will appear around the MPP. However, if the step size is small, the algorithm will minimize the fluctuations around the MPP but the system will slowly track it. In both cases, considerable power will be lost due to the wrong choice of the step size. To overcome the first limitation, many works have been proposed based on conventional INC algorithm with variable step size [26], [27], and [28]. The second shortcoming of conventional INC algorithm lies in the fact that it fails to make the right decision when the solar irradiation changes suddenly from low to high. In this respect, the algorithm increases the duty cycle instead of decreasing it which leads to a loss of power. To overcome this last weakness, some modified INC algorithms have been proposed [29] and [30]. The idea behind these algorithms is to add more conditions to the conventional one.

In this context, the first main contribution in the present paper deals with the design of a new INC MPPT algorithm based on the combination of the two previous techniques. The INC algorithms with variable step and modified INC are used to respectively

overcome the problem of step size choice and ensure the right decision in case of sudden changes of solar irradiation. The second contribution of this work is concerned with the practical implementation of the proposed algorithm using an Arduino board to benefit from its various advantages compared to other microcontrollers and to profit from its easy interfacing with Matlab/Simulink without going through any other programming languages.

The paper is organized as follows: Section 2. is dedicated to the presentation of the PV conversion system modeling and a presentation of the proposed MPPT algorithm. Section 3. is reserved to the discussion of obtained simulation and experimental results. Finally, Sec. 4. concludes the paper.

2. Photovoltaic Conversion System

The overview of the combined PV system is shown in Fig. 1, which mainly consists of a PV panel, a DC-DC boost converter controlled by an MPPT technique and a load.

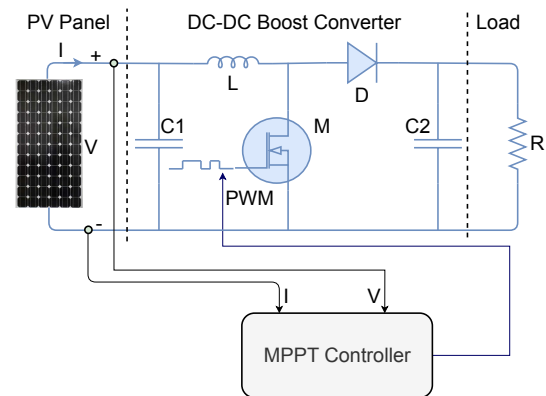


Fig. 1: Block diagram of PV system.

2.1. PV Panel Model

Based on the electrical equivalent circuit model of the PV panel shown in Fig. 2, the PV current can be expressed as [5]:

$$I = n_p I_{ph} - n_p I_s \left(e^{\left[\frac{q(V + R_s I)}{kTA} \right]} - 1 \right) - \frac{V + IR_s}{R_{sh}}, \quad (1)$$

where V , I_s and I_{ph} are the PV output voltage, cell saturation of dark current and light-generated current. R_{sh} and R_s represent the cell shunt and series resistances. The parameters k , q , n_p , T and A repre-

sent the Boltzmann constant, electron charge, number of parallel solar cells, cell temperature and the ideal factor, respectively.

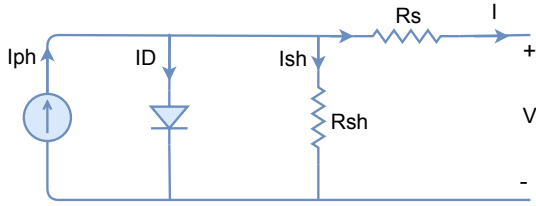


Fig. 2: Electrical equivalent scheme of PV panel.

The light-generated current is expressed as a function of the cell temperature and solar irradiation:

$$I_{ph} = G (I_{sc} + K_I(T - T_r)), \quad (2)$$

where G , T_r and K_I are the solar irradiation in $\text{kW}\cdot\text{m}^{-2}$, cell reference temperature and cell short-circuit current temperature coefficient, respectively. I_{sc} is the cell short-circuit current at 25°C and $1\text{ kW}\cdot\text{m}^{-2}$.

The saturation current can be expressed as a function of the cell temperature, as follows:

$$I_s = I_{rs} \left(\frac{T}{T_r}\right)^3 \exp\left[\frac{qE_g}{kA} \left(\frac{1}{T_r} - \frac{1}{T}\right)\right], \quad (3)$$

where E_g represents the band-gap energy of the semiconductor used in the cell and I_{rs} represents the reverse saturation current which is given by:

$$I_{rs} = \frac{I_{sc}}{\exp\left[\frac{qV_{oc}}{n_s k A T}\right] - 1}, \quad (4)$$

where V_{oc} is the open-circuit voltage.

Figure 3 illustrates the power-voltage and current-voltage characteristics of PV panel. From these plots, it is observed that the variation of the maximum power is highly changed as a function of the cell temperature and solar irradiation.

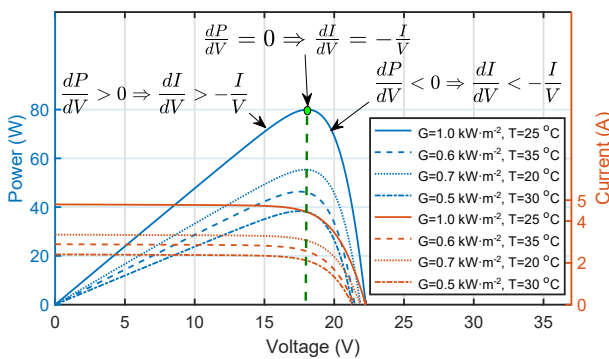


Fig. 3: Nonlinear characteristics of power-voltage and current-voltage.

2.2. Proposed MPPT Algorithm

The conventional INC algorithm is based on the derivative of power with respect to the voltage when the MPP is null. This algorithm uses the conductance value $\left(\frac{I}{V}\right)$ and the incremental conductance value $\left(\frac{dI}{dV}\right)$ to find the MPP. In this respect, the following expression can be obtained:

$$\frac{dP}{dV} = \frac{d(V \cdot I)}{dV} = I \frac{dV}{dV} + V \frac{dI}{dV} = I + V \frac{dI}{dV}. \quad (5)$$

By using the values of both conductance and incremental conductance, the INC algorithm determines the location of the operating point of the PV panel on the power-voltage curve. As shown in Fig. 3, the PV panel operates at the MPP if the condition Eq. (6) is satisfied. In contrast, the PV panel operates on the left side of the MPP if the condition Eq. (7) is satisfied, whereas the PV panel operates on the right side of the MPP if the condition Eq. (8) is satisfied.

$$\frac{dP}{dV} = 0 \Rightarrow \frac{dI}{dV} = -\frac{I}{V}, \quad (6)$$

$$\frac{dP}{dV} > 0 \Rightarrow \frac{dI}{dV} > -\frac{I}{V}, \quad (7)$$

$$\frac{dP}{dV} < 0 \Rightarrow \frac{dI}{dV} < -\frac{I}{V}. \quad (8)$$

The flowchart of the conventional INC algorithm is illustrated in Fig. 4(a). During the operating points, the INC algorithm perturbs the system and increases the duty ratio (D) with a fixed step (dD) when the sign of the $\frac{dP}{dV}$ is positive. Otherwise, if the sign of $\frac{dP}{dV}$ is negative, the algorithm perturbs the system in the opposite direction and decreases the duty ratio. However, the conventional INC algorithm suffers from several drawbacks. The first one resides in the choice of step size. Therefore, many INC algorithms have been proposed where the step size (dD) is given as a function of dP , as follows:

$$dD = N \cdot |dP|, \quad (9)$$

where N is a scaling factor.

Another drawback of the conventional INC algorithm resides in the fact that if condition Eq. (6) is satisfied, then there is nothing to do, and in this case, the duty cycle is fixed and no oscillation occurs. However, this condition is rarely satisfied in real conditions because of the truncation error of the numerical differentiation. Moreover, the conventional INC algorithm fails to make the right decision when the solar irradiation changes suddenly. To overcome these drawbacks, some modified INC algorithms have been proposed. The idea behind these algorithms is to check

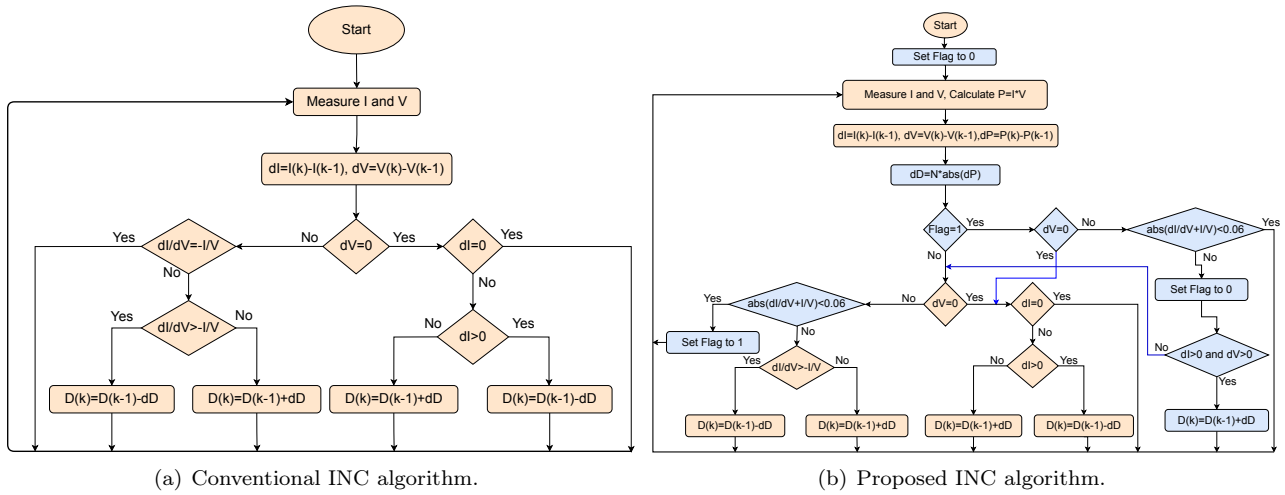


Fig. 4: Flowcharts of conventional and proposed INC algorithms.

if the MPP is met with increases in both current and voltage, in this case, the permitted error Eq. (10) is applied to verify that the MPP is reached.

$$\left| I + V \frac{dI}{dV} \right| < 0.06. \quad (10)$$

In this work, a combined methodology of both algorithms is proposed using the principle of variable step size to overcome the drawback of step size choice. In addition, it uses a permitted error to verify that the algorithm takes the right decision when the solar irradiation increases suddenly. The flowchart of the proposed INC algorithm is shown in Fig. 4(b).

3. Results and Discussion

3.1. Simulation Results

In order to verify the validity and effectiveness of the proposed modified incremental conductance algorithm, simulation tests have been carried out on a PV system using the Simulink model shown in Fig. 5 and the parameters given in Tab. 1.

Note that during the simulation tests, the proposed INC algorithm is compared with the conventional one with a fixed step size of 0.005.

The first simulation test is carried out in various atmospheric conditions. The solar irradiation and cell temperature profiles are assumed to be as shown in Fig. 6(a) and Fig. 6(b), respectively. The responses of PV output power and PV output current are shown in Fig. 6(c) and Fig. 6(d), while the responses of the PV output voltage and the control signal are shown in Fig. 6(e) and Fig. 6(f). It is evident that the proposed INC algorithm has more

efficiency than conventional one at different levels of irradiation and temperature, most notably when the irradiation increases or decreases. Moreover, portions of the steady states in different ranges are enlarged to show the efficiency of the proposed MPPT algorithm. It can clearly be seen from the enlarged portions that the responses of steady states with the proposed INC method track perfectly their optimum operating points with much less oscillation, whereas the responses of PV system with the conventional INC method show a considerable amount of oscillation in the different states. This improves the efficiency and greatly reduces the PV power loss.

Tab. 1: PV conversion system parameters.

| Symbol | Quantity | Value |
|-----------|-------------------------------|--|
| P_r | Rated Power | 80 W |
| k | Boltzmann's constant | $1.38 \cdot 10^{23} \text{ J} \cdot \text{K}^{-1}$ |
| A | Ideal factor of PV-Cell | 1.1 |
| R_{sh} | Shunt resistance | 360.002 Ω |
| R_s | Series resistance | 0.18 Ω |
| n_s | Cells connected in series | 36 |
| n_p | Number of module in parallel | 1 |
| T_0 | Temperature reference | 298.15 K |
| G_0 | Irradiation reference | 1000 $\text{W} \cdot \text{m}^{-2}$ |
| V_{oc} | Open-circuit Voltage | 22 V |
| I_{sc} | Short-circuit current | 4.8 A |
| I_{scn} | Nominal short-circuit current | 4.45 A |
| V_{pvn} | Nominal PV voltage | 18 V |

The second simulation test is conducted with a stable temperature at $T = 25^\circ\text{C}$, but the solar irradiation profile is assumed to be as shown in Fig. 7(a). This test is carried out to evaluate the proposed and traditional algorithms in case of triangular changes of solar irradiation. The response of PV power is illustrated in Fig. 7(b). It is clearly shown that the proposed algorithm has superior performance in term of tracking compared to the conventional one.

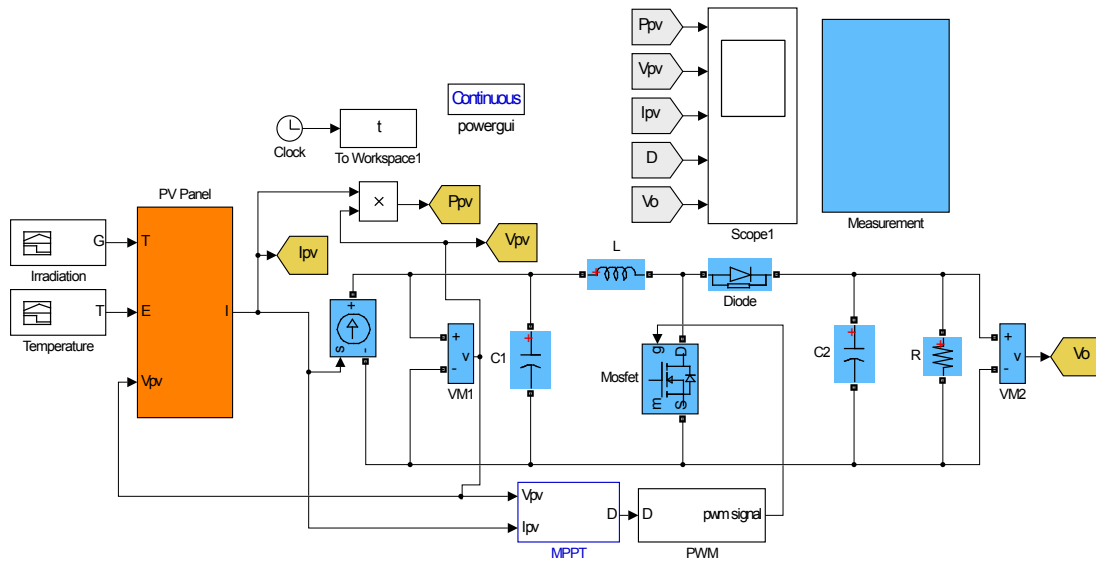


Fig. 5: Model of PV system using Simulink.

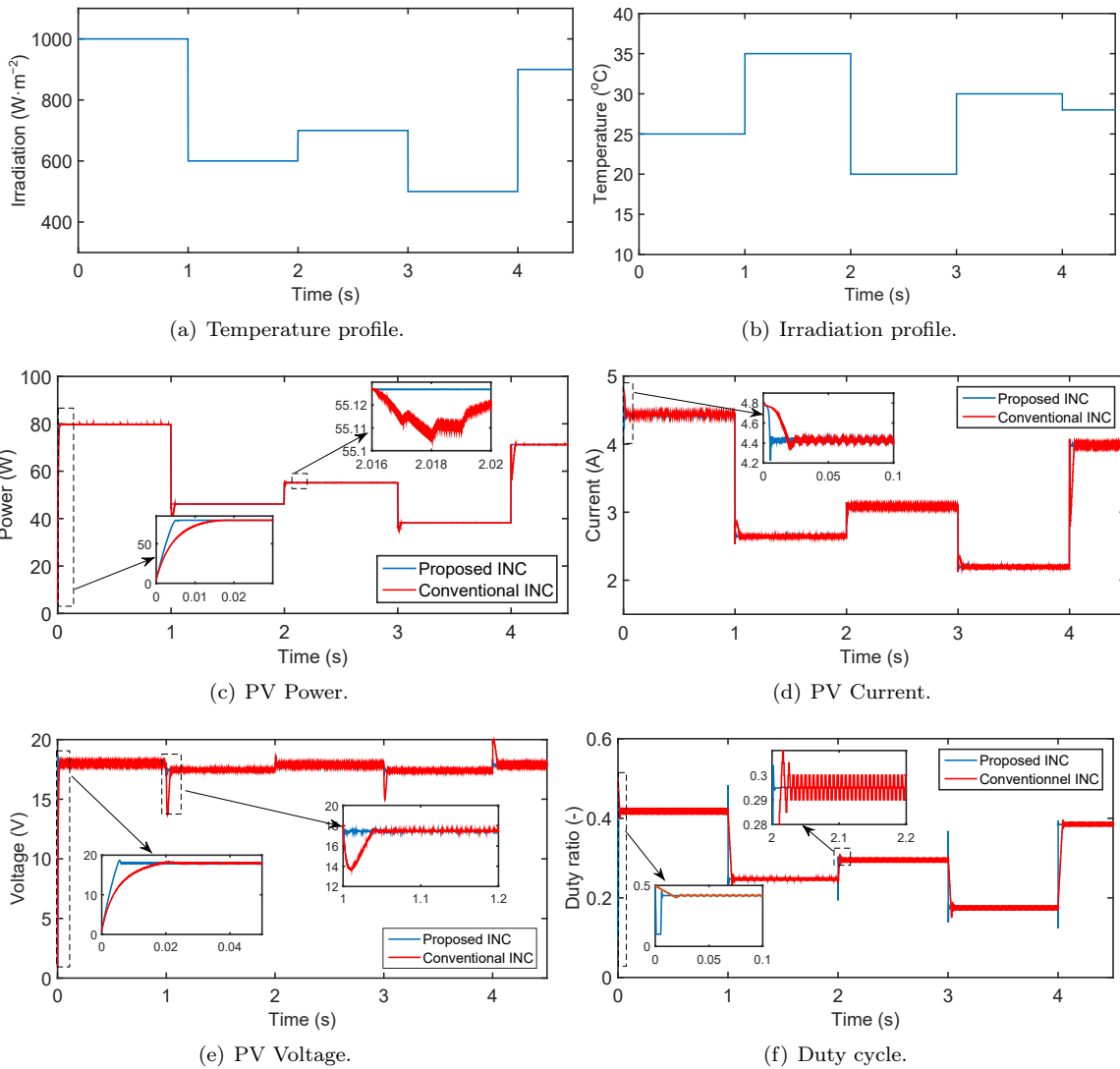
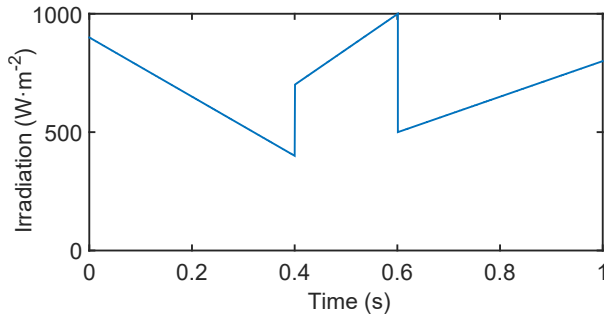
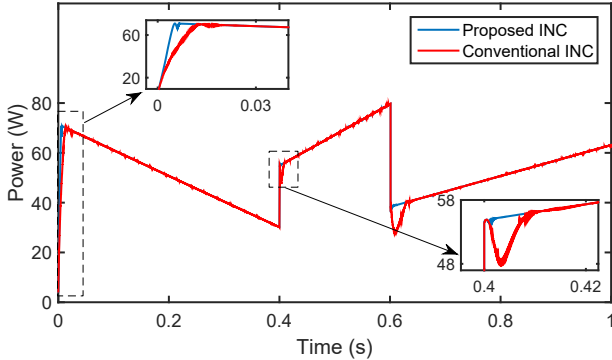


Fig. 6: Simulation results for PV system under varying environmental conditions.



(a) Irradiation profile.



(b) PV power.

Fig. 7: Simulation results for PV system under a droop change in the irradiation.

The last simulation test is carried out to evaluate the proposed and conventional algorithms in case of sudden change in load at a specific time. The environmental conditions are assumed to be constant ($G = 1 \text{ kW}\cdot\text{m}^{-2}$ and $T = 25 \text{ }^\circ\text{C}$). The resistance load is assumed to be firstly equal to $100 \text{ }\Omega$, and then suddenly changed to be equal to $50 \text{ }\Omega$ at time $t = 0.5 \text{ s}$. Figure 8 shows clearly that the response of PV power with the proposed INC method track perfectly its maximum point with much less fluctuation, whereas the response of PV power with the conventional INC method shows a considerable amount of fluctuation especially during the sudden change of the load.

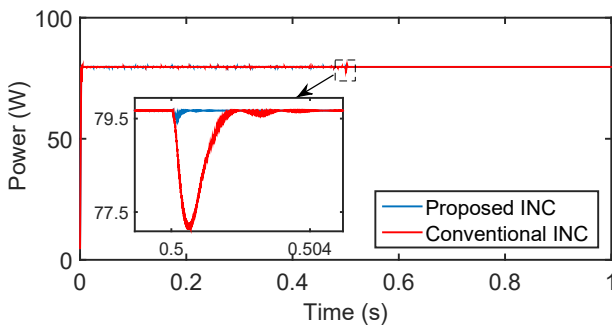


Fig. 8: Responses of power under load variation at $t = 0.5 \text{ s}$.

In addition to these simulation tests, some other tests are considered using different indices describing

the behaviours of the proposed and compared algorithms during static and dynamic changes. These indices are given as follows [31]:

Accuracy a_{MPPT} : This index is used to know how close is the tracking to the maximum point. In our study, it was used to illustrate how close is the PV current during tracking to the current maximum power point, as given below:

$$a_{MPPT} = \frac{I_{pv}}{I_{MPPT}} \cdot 100. \quad (11)$$

Static efficiency index η_{MPPT} shows the ratio of actual PV power to the maximum power. It is given by:

$$\eta_{MPPT} = \frac{P_{pv}}{P_{MPP}} \cdot 100. \quad (12)$$

Relative tracking error (ε_{MPPT}) is expressed as follows:

$$\varepsilon_{MPPT} = \left| \frac{P_{pv}}{P_{MPP}} - 1 \right| \cdot 100. \quad (13)$$

In addition, the indices Eq. (14) and Eq. (15) which represent the MPPT energetic efficiency and the MPPT energetic error, respectively, are used to evaluate the tracking performance of the proposed and conventional algorithms during dynamic changes in the MPP [31].

$$\eta_{MPPT,E} = \left(\frac{\int_0^{t_f} P_{pv} dt}{\int_0^{t_f} P_{MPP} dt} \right) \cdot 100, \quad (14)$$

$$\varepsilon_{MPPT,E} = \left(\frac{\int_0^{t_f} P_{pv} dt}{\int_0^{t_f} P_{MPP} dt} - 1 \right) \cdot 100. \quad (15)$$

Table 2 shows the values of considered indices for the proposed and conventional MPPT algorithms. It is clearly demonstrated that the proposed modified INC algorithm based on variable step size guarantees better performance compared to the conventional one.

Tab. 2: Performances comparison between the proposed and conventional INC algorithms.

| Index | Proposed INC | Conventional INC |
|------------------------|--------------|------------------|
| a_{MPPT} | 98.4101 | 97.6449 |
| η_{MPPT} | 98.2547 | 97.1643 |
| ε_{MPPT} | 1.3937 | 2.9671 |
| $\eta_{MPPT,E}$ | 98.4292 | 97.3918 |
| $\varepsilon_{MPPT,E}$ | 1.4768 | 2.8768 |

From the analysis of the previous results, it can clearly be seen that the proposed INC algorithm has

higher tracking speed and offers better performances than the conventional one in terms of efficiency and power quality.

3.2. Experimental Results

The main purpose of this section is to experimentally validate the developed algorithm using Arduino Mega board with Matlab/Simulink environment, as shown in Fig. 9. The implementation stage includes two parts:

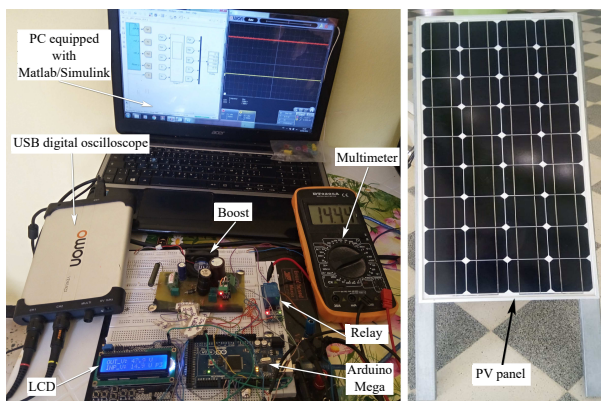


Fig. 9: Hardware setup for PV system.

The **Hardware part** consists of a boost converter, a PV panel of 80 W, a resistive load, relay and an LCD which displays the different measured signals. In addition, a USB digital oscilloscope and digital multimeter are used to verify the acquired signals.

The considered DC-DC boost converter in this work consists of an input capacitor, an input current sensor, a potentiometer used as an input voltage sensor, an inductor, a MOSFET switch, a diode, an output capacitor, a potentiometer used as an output voltage sensor and a resistive load. Figure 10 shows the real hardware implementation of the considered boost converter using the parameters shown in Tab. 3.

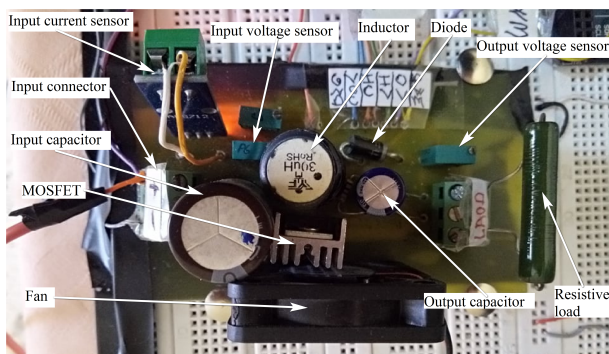


Fig. 10: Boost converter prototype.

Tab. 3: DC-DC boost converter parameters.

| Symbol | Value |
|---------------------|--------------|
| Inductor | 30 μ H |
| Input capacitor | 1000 μ F |
| Output capacitor | 470 μ F |
| Resistor load | 56 Ω |
| Switching frequency | 31.4 kHz |
| MOSFET | IRFZ44N |
| Ultrafast Diode | 31DF4 |

Software part: In this work, Matlab/Simulink environment is used to associate the hardware setup with the Arduino board. This solution allows to benefit from the various advantages of this board which can easily interface with Matlab/Simulink directly without going through any other programming languages thanks to many special packages such as “Simulink support package for Arduino hardware”. This package creates library blocks in Simulink that allow configuring and accessing Arduino sensors and communication interfaces. It also enables to interactively monitor and tune algorithms developed in Simulink as they run, in real-time, on the Arduino.

Figure 11 illustrates the Simulink model used for the implementation of the developed MPPT algorithm. The Simulink model is composed mainly of eight blocks. The first one designated as “From PV current sensor” is reserved to acquire the PV current via the analog pin 14. The second and third blocks indicated “From PV voltage sensor” and “From output sensor” are reserved to acquire the PV voltage and load voltage via the analog pins 15 and 13. The fourth block mentioned as “MPPT algorithm” is dedicated to the implementation of the proposed algorithm which generates the appropriate duty cycle and then sends it to the DC-DC boost converter using the fifth block “PWM” via the analog pin 9. The sixth block mentioned as “step” is used to control the starting record data at time $t = 0.1$ s by sending a digital signal to the relay using the seventh block designated as “Relay control” via the digital pin 2.

The “S-function” block is a builder, which is a computer language description of a Simulink block written in “C” programming language. This block is mainly used for the following reasons:

- to calculate the average of 200 acquired current and voltage values to reduce the noise during the data acquisition process (noise filter), as shown in Fig. 12;
- to show on the LCD the different values of the acquired signals, as illustrated in Fig. 13;

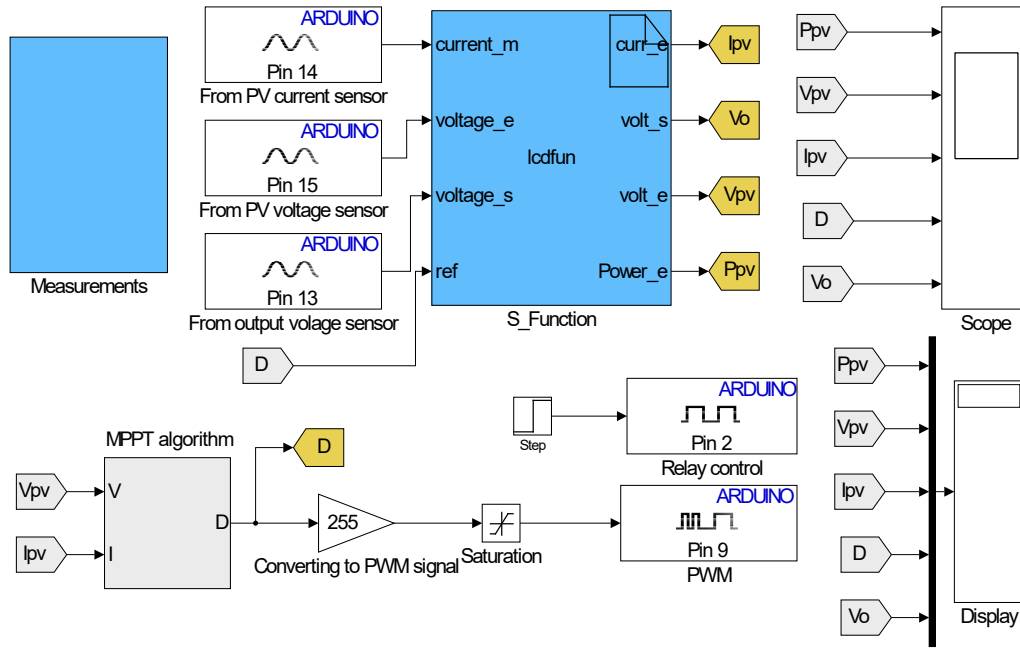


Fig. 11: Simulink model used for real-time implementation.

```

S-Function Builder: INC_vss_MPPPT_Arduino_2019_3/LCD Display
Port/Parameter:
Input Ports
  current_m
  voltage_e
  voltage_s
  ref
Output Ports
  curr_e
  volt_s
  volt_e
  Power_e
Parameters

Code description
Enter your C-code or call your algorithm. If available, discrete and continuous states should be referenced as,
xD[0]...xD[n], xC[0]...xC[n] respectively. Input ports, output ports and parameters should be referenced using the
symbols specified in the Data Properties. These references appear directly in the generated S-function.

if (xD[0] == 1)
{
    #ifndef MATLAB_MEX_FILE
    curr_e[0]=0;
    volt_s[0]=0;
    volt_e[0]=0;
    //Output Voltage
    for(int i = 0; i < 199; i++) (volt_e[i]= volt_e[i]+(voltage_e[i]* 0.0594));
    //Input Voltage
    for(int i = 0; i < 199; i++) (volt_e[i]= volt_e[i]+(voltage_e[i]* 0.026));
    //Input Current
    for(int i = 0; i < 199; i++) (curr_e[i]=curr_e[i] +(current_m[i] - 504)*0.04);
    volt_s[0]=volt_s[0]/200; volt_e[0]=volt_e[0]/200; curr_e[0]=curr_e[0]/200;
    //Power
    power=volt_e[0]*curr_e[0];
}
Inputs are needed in the output function(direct feedthrough)
    
```

Fig. 12: C-code used to calculate the acquired signals.

```

S-Function Builder: INC_vss_MPPPT_Arduino_2019_3/LCD Display
Port/Parameter:
Input Ports
  current_m
  voltage_e
  voltage_s
  ref
Output Ports
  curr_e
  volt_s
  volt_e
  Power_e
Parameters

Code description
This section is optional and use to update the discrete states. It is called only if the S-function has one or more
discrete states. The states of the S-function are of type double and must be referenced as xD[0], xD[1], etc. respectively.
Input ports, output ports and parameters should be referenced using the symbols specified in the Data Properties. These
references appear directly in the generated S-function.

if (xD[0] != 1)
{
    #ifndef MATLAB_MEX_FILE
    TCCR2B = TCCR2B & B11110000 | B00000001; // Changing frequency to 31.372.55 Hz
    ICR2 = 16;
    #endif
    xD[0] = 1;
}
    
```

Fig. 14: C-code used to change the frequency.

```

S-Function Builder: INC_vss_MPPPT_Arduino_2019_3/LCD Display
Port/Parameter:
Input Ports
  current_m
  voltage_e
  voltage_s
  ref
Output Ports
  curr_e
  volt_s
  volt_e
  Power_e
Parameters

Code description
Enter your C-code or call your algorithm. If available, discrete and continuous states should be referenced as,
xD[0]...xD[n], xC[0]...xC[n] respectively. Input ports, output ports and parameters should be referenced using the
symbols specified in the Data Properties. These references appear directly in the generated S-function.

if (digitalRead(pb4) == LOW) (delay(10); while (digitalRead(pb4) == LOW); count++)
if (count < 0) count = 0;
switch (count)
{
    case 0:
        lcd.clear(); lcd.setCursor(0,0); lcd.print("IMP_Vv: "); lcd.setCursor(7,0); lcd.print(vo);
        lcd.setCursor(12,0); lcd.print(" V"); lcd.setCursor(0,1); lcd.print("IMP_Ci: "); lcd.setCursor(7,1);
        lcd.print(curr_e[0]); lcd.setCursor(11,1); lcd.print(" A"); lcd.setCursor(14,1); lcd.print(" ");
        break;
    case 1:
        lcd.clear(); lcd.setCursor(0,0); lcd.print("Power: "); lcd.setCursor(7,0); lcd.print(Po);
        lcd.setCursor(0,1); lcd.print(" W"); lcd.setCursor(0,1); lcd.print("DutyC: "); lcd.setCursor(7,1);
        lcd.print(" "); lcd.setCursor(14,1); lcd.print(" %");
        break;
}
Inputs are needed in the output function(direct feedthrough)
    
```

Fig. 13: Part of the C-code used to programming the LCD.

- to increase the default frequency of pin 9 from 490 Hz to the required frequency 31.4 kHz by using the C-code mentioned in Fig. 14.

In order to show the better quality of the proposed algorithm in terms of time response and power exactation, experimental tests of the proposed and conventional INC algorithms are carried out On April 18th,

2020 in Tebessa-Algeria, where the solar irradiation was almost $647 \text{ W} \cdot \text{m}^{-2}$ and the temperature was $28 \text{ }^\circ\text{C}$. The experimental waveforms of PV power and PV current are shown in Fig. 15(a) and Fig. 15(b), while the experimental waveforms of the PV voltage and duty cycle are shown in Fig. 15(c) and Fig. 15(d). From these experimental results, it can be seen that both algorithms yield good results in terms of rapidity, but the responses of the steady states with the proposed modified INC track perfectly their optimum operating points with much less fluctuation, while the responses of the PV system with the conventional INC show a considerable amount of oscillation in the different states. These results confirmed the experimental validity of the proposed technique as well as its superiority to the classical one.

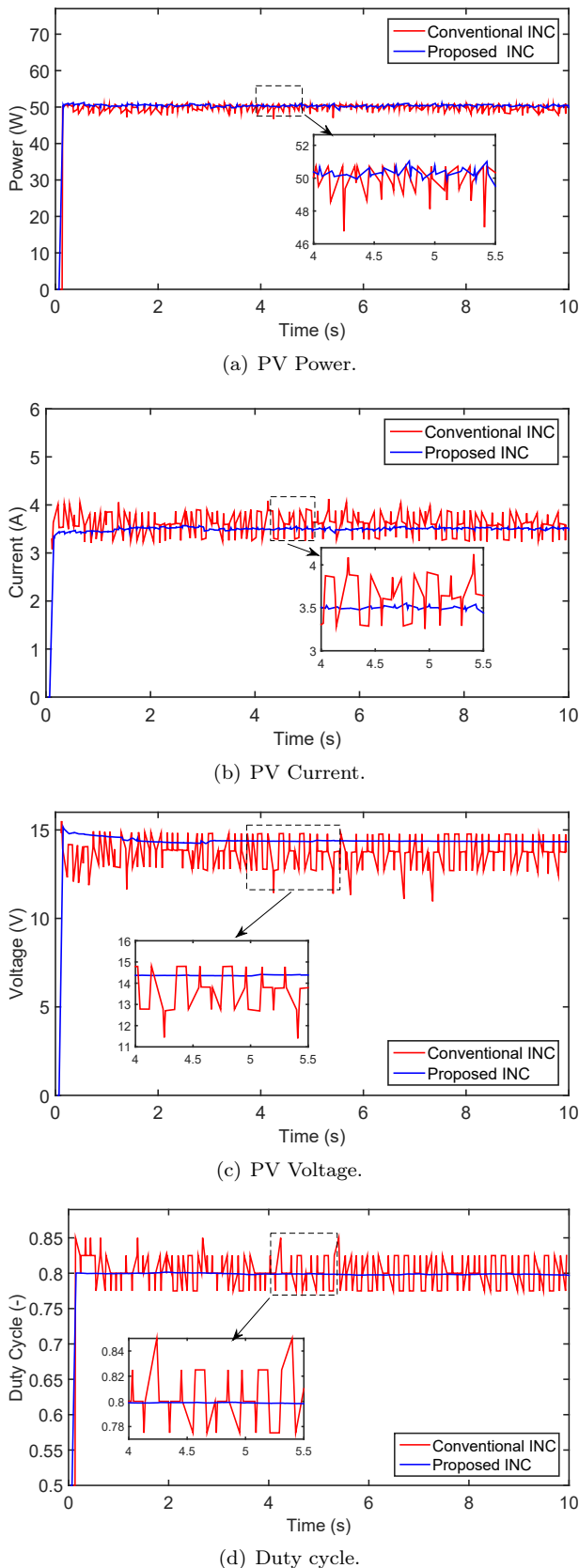


Fig. 15: Experimental results for PV system under solar irradiation $G = 647 \text{ W}\cdot\text{m}^{-2}$ and temperature $T = 28 \text{ }^\circ\text{C}$.

4. Conclusion

A new modified incremental conductance algorithm is proposed for maximum power point tracking for a photovoltaic system. The simulation results clearly show that the proposed method can quickly converge to the maximum power point with much less oscillation during rapid changes of atmospheric conditions, and has a high power output efficiency compared to the conventional method. The experimental validation of the proposed and conventional algorithms is conducted using an Arduino mega board and a special Matlab/Simulink package known as a Simulink support package for Arduino hardware. The experimental results show the validity of the proposed method and its superior performance compared to the conventional method, in term of convergence to the MPP with much less oscillations.

Author Contributions

O.D. conceptualized the idea of the research and also carried out the analytical modelling and simulation. O.D. and G.D. contributed to the design and hardware implementation of the research. O.D., G.D. and S.Y. contributed to the analysis of the simulation and experimental results. M.M. developed the PCB design and manufacturing of the DC-DC boost converter. All authors discussed the results and commented on the manuscript. All authors involved in analyzing, drafting, and editing of the paper.

References

- [1] YADAV, I., S. K. MAURYA and G. K. GUPTA. A Literature Review on Industrially Accepted MPPT Techniques for Solar PV System. *International Journal of Electrical and Computer Engineering*. 2020, vol. 10, iss. 2, pp. 2117–2127. ISSN 2088-8708. DOI: 10.11591/ijece.v10i2.pp2117-2127.
- [2] REPAK, M., A. OTCENASOVA, J. ALTUS and M. Regula. Grid-tie power converter for model of photovoltaic power plant. *Electrical Engineering*. 2017, vol. 99, iss. 4, pp. 1377–1391. ISSN 0948-7921. DOI: 10.1007/s00202-017-0611-6.
- [3] DEPURU, S. R. and M. MAHANKALI. Boost Converter Fed High Performance BLDC Drive for Solar PV Array Powered Air Cooling System. *Advances in Electrical and Electronic Engineering*. 2017, vol. 15, iss. 2, pp. 154–168. ISSN 1804-3119. DOI: 10.15598/aeee.v15i2.2133.

- [4] LATKOVA, M., M. BAHERNIK, M. HOGER and P. BRACINIK. FSM Model of a Simple Photovoltaic System. *Advances in Electrical and Electronic Engineering*. 2015, vol. 13, iss. 3, pp. 230–235. ISSN 1804-3119. DOI: 10.15598/aeee.v13i3.1411.
- [5] OUNNAS, D., M. RAMDANI, S. CHENIKHER and T. BOUKTIR. An Efficient Maximum Power Point Tracking Controller for Photovoltaic Systems Using Takagi–Sugeno Fuzzy Models. *Arabian Journal for Science and Engineering*. 2017, vol. 42, iss. 12, pp. 4971–4982. ISSN 2191-4281. DOI: 10.1007/s13369-017-2532-0.
- [6] BOUNECHBA, H., A. BOUZID, H. SNANI and A. LASHAB. Real time simulation of MPPT algorithms for PV energy system. *International Journal of Electrical Power and Energy Systems*. 2016, vol. 83, iss. 1, pp. 67–78. ISSN 0142-0615. DOI: 10.1016/j.ijepes.2016.03.041.
- [7] RAHMANI, B., W. LI and G. LIU. An Advanced Universal Power Quality Conditioning System and MPPT method for grid integration of photovoltaic systems. *International Journal of Electrical Power and Energy Systems*. 2015, vol. 69, iss. 1, pp. 76–84. ISSN 0142-0615. DOI: 10.1016/j.ijepes.2014.12.031.
- [8] VERMA, D., S. NEMA, A. M. SHANDILYA and S. K. DASH. Maximum power point tracking (MPPT) techniques: Recapitulation in solar photovoltaic systems. *Renewable and Sustainable Energy Reviews*. 2016, vol. 54, iss. 1, pp. 1018–1034. ISSN 1364-0321. DOI: 10.1016/j.rser.2015.10.068.
- [9] XIAO, X., X. HUANG and Q. KANG. A Hill-Climbing-Method-Based Maximum-Power-Point-Tracking Strategy for Direct-Drive Wave Energy Converters. *IEEE Transactions on Industrial Electronics*. 2015, vol. 63, iss. 1, pp. 257–267. ISSN 1557-9948. DOI: 10.1109/TIE.2015.2465964.
- [10] LIU, H.-D, C.-H. LIN, K.-J. PAI and Y.-L. LIN. A novel photovoltaic system control strategies for improving hill climbing algorithm efficiencies in consideration of radian and load effect. *Energy Conversion and Management*. 2018, vol. 165, iss. 1, pp. 815–826. ISSN 0196-8904. DOI: 10.1016/j.enconman.2018.03.081.
- [11] AHMED, J. and Z. SALAM. An improved perturb and observe (P&O) maximum power point tracking (MPPT) algorithm for higher efficiency. *Applied Energy*. 2015, vol. 150, iss. 1, pp. 97–108. ISSN 0306-2619. DOI: 10.1016/j.apenergy.2015.04.006.
- [12] TAJUDDIN, M. F. N., M. S. ARIF, S. M. AYOB and Z. SALAM. Perturbative methods for maximum power point tracking (MPPT) of photovoltaic (PV) systems: a review. *International Journal of Energy Research*. 2015, vol. 39, iss. 1, pp. 1153–1178. ISSN 0363-907X. DOI: 10.1002/er.3289.
- [13] ZAKZOUK, N. E., M. A. ELSAHARTY, A. K. ABDELSALAM, A. A. HELAL and B. W. WILLIAMS. Improved performance low cost incremental conductance PV MPPT technique. *IET Renewable Power Generation*. 2016, vol. 10, iss. 4, pp. 561–574. ISSN 1752-1416. DOI: 10.1049/iet-rpg.2015.0203.
- [14] SIVAKUMAR, P., A. A. KADER, Y. KALI-AVARADHAN and M. ARUTCHELVI. Analysis and enhancement of PV efficiency with incremental conductance MPPT technique under non-linear loading conditions. *Renewable Energy*. 2015, vol. 81, iss. 1, pp. 543–550. ISSN 0960-1481. DOI: 10.1016/j.renene.2015.03.062.
- [15] BATAINEH, K. and N. EID. A Hybrid Maximum Power Point Tracking Method for Photovoltaic Systems for Dynamic Weather Conditions. *Resources*. 2018, vol. 7, iss. 4, pp. 68–83. ISSN 2079-9276. DOI: 10.3390/resources7040068.
- [16] EYDI, M., S. I. HOSSEINI SABZEVARI and R. GHAZI. A Novel Strategy of Maximum Power Point Tracking for Photovoltaic Panels Based on Fuzzy Logic Algorithm. *Advances in Electrical and Electronic Engineering*. 2020, vol. 18, iss. 1, pp. 25–35. ISSN 1804-3119. DOI: 10.15598/aeee.v18i1.3511.
- [17] ALDAIR, A. A., A. A. OBED and A. F. HAL-IHAL. Design and implementation of ANFIS-reference model controller based MPPT using FPGA for photovoltaic system. *Renewable and Sustainable Energy Reviews*. 2018, vol. 82, iss. 1, pp. 2202–2217. ISSN 1364-0321. DOI: 10.1016/j.rser.2017.08.071.
- [18] MLAKIC, D., L. MAJDANDZIC and S. NIKOLOVSKI. ANFIS Used as a Maximum Power Point Tracking Algorithm for a Photovoltaic System. *International Journal of Electrical and Computer Engineering*. 2018, vol. 8, iss. 2, pp. 867–879. ISSN 2088-8708. DOI: 10.11591/ijece.v8i2.pp867-879.
- [19] OMAR, O. A. M., N. M. BADRA and M. A. ATTIA. Enhancement of On-grid PV System under Irradiance and Temperature Variations Using New Optimized Adaptive Controller. *International Journal of Electrical and Computer Engineering*.

- 2018, vol. 8, iss. 5, pp. 2650–2660. ISSN 2088-8708. DOI: 10.11591/ijece.v8i5.pp2650-2660.
- [20] MOHAMED, A. A. S., A. BERZOY and O. A. MOHAMMED. Design and Hardware Implementation of FL-MPPT Control of PV Systems Based on GA and Small-Signal Analysis. *IEEE Transactions on Sustainable Energy*. 2016, vol. 8, iss. 1, pp. 279–290. ISSN 1949-3037. DOI: 10.1109/TSTE.2016.2598240.
- [21] FATHY, A., I. ZIEDAN and D. AMER. Improved teaching–learning-based optimization algorithm-based maximum power point trackers for photovoltaic system. *Electrical Engineering*. 2018, vol. 100, iss. 3, pp. 1773–1784. ISSN 1432-0487. DOI: 10.1007/s00202-017-0654-8.
- [22] EL MALAH, M., A. BA-RAZZOUK, M. GUISSER, E. ABDELMOUNIM and M. MADARK. Backstepping based power control of a three-phase single-stage grid-connected PV system. *Electrical Engineering*. 2019, vol. 9, iss. 6, pp. 4738–4748. ISSN 2088-8708. DOI: 10.11591/ijece.v9i6.pp4738-4748.
- [23] WU, Z., D. YU, DANQI and X. KANG. Application of improved chicken swarm optimization for MPPT in photovoltaic system. *Optimal Control Applications and Methods*. 2018, vol. 39, iss. 2, pp. 1029–1042. ISSN 1099-1514. DOI: 10.1002/oca.2394.
- [24] SOUFI, Y., M. BECHOUAT and S. KAHLA. Fuzzy-PSO controller design for maximum power point tracking in photovoltaic system. *International Journal of Hydrogen Energy*. 2017, vol. 42, iss. 13, pp. 8680–8688. ISSN 0360-3199. DOI: 10.1016/j.ijhydene.2016.07.212.
- [25] DEPURU, S. R. and M. MAHANKALI. Performance Analysis of a Maximum Power Point Tracking Technique using Silver Mean Method. *Advances in Electrical and Electronic Engineering*. 2018, vol. 16, iss. 1, pp. 25–35. ISSN 1804-3119. DOI: 10.15598/aece.v16i1.2249.
- [26] SINGH, P., N. SHUKLA and P. GAUR. Modified variable step incremental-conductance MPPT technique for photovoltaic system. *International Journal of Information Technology*. 2020, pp. 1–8. ISSN 2511-2112. DOI: 10.1007/s41870-020-00450-8.
- [27] NECAIBIA, S., M. S. KELAIAIA, H. LABAR, A. NECAIBIA and E. D. CASTRONOVO. Enhanced auto-scaling incremental conductance MPPT method, implemented on low-cost micro-controller and SEPIC converter. *Solar Energy*. 2019, vol. 180, iss. 1, pp. 152–168. ISSN 0038-092X. DOI: 10.1016/j.solener.2019.01.028.
- [28] MIRZA, A. F., M. MANSOOR, Q. LING, M. I. KHAN and O. M. ALDOSSARY. Advanced Variable Step Size Incremental Conductance MPPT for a Standalone PV System Utilizing a GA-Tuned PID Controller. *Energies*. 2020, vol. 13, iss. 16, pp. 41–52. ISSN 1996-1073. DOI: 10.3390/en13164153.
- [29] MOTAHHIR, S., A. EL GHZIZAL, S. SEBTI and A. DEROUICH. Modeling of Photovoltaic System with Modified Incremental Conductance Algorithm for Fast Changes of Irradiance. *International Journal of Photoenergy*. 2018, vol. 2018, iss. 1, pp. 1–14. ISSN 1687-529X. DOI: 10.1155/2018/3286479.
- [30] XIAO, W., W. G. DUNFORD, P. R. PALMER and A. CAPEL. Application of Centered Differentiation and Steepest Descent to Maximum Power Point Tracking. *IEEE Transactions on Industrial Electronics*. 2007, vol. 54, iss. 5, pp. 2539–2549. ISSN 1557-9948. DOI: 10.1109/TIE.2007.899922.
- [31] MOUSSA, A. G. E., S. H. E. A. ALEEM and A. M. IBRAHIM. Mathematical Analysis of Maximum Power Points and Currents Based Maximum Power Point Tracking in Solar Photovoltaic System: a Solar Powered Water Pump Application. *International Review of Electrical Engineering*. 2016, vol. 11, iss. 1, pp. 97–108. ISSN 1827-6660. DOI: 10.15866/iree.v11i1.8137.

About Authors

Djamel OUNNAS was born in Tebessa, Algeria. He received a B.Sc. degree in electronics engineering from Tebessa University, Algeria in 2007, Magister degree in automatic from Biskra University in 2011 and Ph.D. degree in Automatic from Setif University, Algeria in 2016. Currently he is a Professor in the department of Electrical Engineering, Larbi Tebessi University, Tebessa, Algeria. His research interests include fault detection and diagnosis in industrial systems, fuzzy control of electrical drives, energy conversion and power control.

Dhaouadi GUIZA was born in Tebessa, Algeria. He received a B.Sc. degree in Electronics from Skikda University, Algeria in 2001, Magister degree in electronic components and system from Constantine University, Algeria in 2009 and Ph.D. degree in Electronic from Skikda University, Algeria in 2020. His research interests include fuzzy control of electrical drives, energy conversion and power control, practical electronics and Drives.

Youcef SOUFI was born in Tebessa, Algeria. He received a B.Sc. degree from the University of Annaba, Algeria, in 1991, Magister degree in Electrical Engineering from Tebessa University, Algeria in 1997 and Ph.D. degree in Automatic from Annaba University, Algeria in 2012. Currently, he is a Professor in the department of Electrical Engineering, Tebessa, Algeria. His research interests include electrical machines control and drives applied to renewable and sustainable energy.

Mahmoud MAAMRI was born in Tebessa, Algeria. He received a B.Sc. degree from the University of Annaba, Algeria, in 1987, Magister degree in in electromechanical engineering from Skikda University, Algeria in 1991 and Ph.D. degree in Electronic from Annaba University, Algeria in 2004. Currently, he is a Professor in the department of Electrical Engineering, Tebessa, Algeria. His main research fields include electrical machines, control systems and renewable energy.